BIOPHARMACEUTICS & DRUG DISPOSITION
Biopharm. Drug Dispos. **28**: 349–360 (2007)
Published online in Wiley InterScience
(www.interscience.wiley.com) **DOI**: 10.1002/bdd.562

Pharmacokinetic Modelling of Blood–Brain Barrier Transport of Escitalopram in Rats

Christoffer Bundgaard[a,*], Martin Jørgensen[b] and Frank Larsen[c]
[a] *Discovery ADME, H. Lundbeck A/S, 9 Ottiliavej, DK-2500 Valby, Denmark*
[b] *Early Development Pharmacokinetics, H. Lundbeck A/S, 9 Ottiliavej, DK-2500 Valby, Denmark*
[c] *Clinical Pharmacology and Pharmacokinetics, H. Lundbeck A/S, 9 Ottiliavej, DK-2500 Valby, Denmark*

ABSTRACT: This study examined the pharmacokinetics and distribution of escitalopram in the brain extracellular fluid in rats by the concurrent use of intracerebral microdialysis and serial blood sampling. Following three constant intravenous infusions, drug concentrations in the hippocampus and plasma were monitored for 6 h. To estimate the integrated pharmacokinetics and intercompartmental transport parameters, including blood–brain barrier (BBB) transport over the entire dose range, unbound brain and plasma escitalopram concentration data from all doses were simultaneously analysed using compartmental modelling. The pharmacokinetic analysis revealed that systemic clearance decreased as a function of dose, which was incorporated in the integrated model. Escitalopram was rapidly and extensively transported across the BBB and distributed into the brain extracellular fluid. The modelling resulted in an estimated influx clearance into the brain of 535 μl/min/g brain, resulting in an unbound brain-to-plasma *AUC* ratio of 0.8 independent of escitalopram dose. The model may be applied for preclinical evaluations or predictions of escitalopram concentration-time courses in plasma as well as at the target site in the CNS for various dosing scenarios. In addition, this modelling approach may also be valuable for studying BBB transport characteristics for other psychotropic agents.

Key words: blood–brain barrier; escitalopram; microdialysis; modelling; pharmacokinetics

Introduction

Escitalopram is a serotonin dual action antidepressant that binds both to the primary site on the serotonin transporter, and to an allosteric site that has been shown to augment the efficiency of serotonin reuptake. This serotonin dual action is thought to be responsible for the superior efficacy of escitalopram compared with conventional selective serotonin reuptake inhibitors (SSRIs) for the treatment of major depressive disorder and anxiety disorders [1–3]. Escitalopram has also shown potent efficacy in a variety of *in vivo* pharmacological animal models predictive of antidepressant and anxiolytic activities [4–6]. However, as is the case for other antidepressant compounds, limited information is available regarding drug concentrations at the site of action in the central nervous system (CNS) and the pharmacokinetic interrelationship between blood and brain. Accordingly, drug exposure measurements are typically performed in easily accessible physiological compartments such as blood or plasma, which may not appropriately reflect the concentration in the CNS, especially during the non steady-state conditions following acute administration [7,8].

*Correspondence to: Discovery ADME, H. Lundbeck A/S, 9 Ottiliavej, DK-2500 Valby, Denmark. E-mail: cbun@lundbeck.com

Received 10 October 2006
Revised 4 March 2007
Accepted 6 March 2007

Even if brain tissue homogenates are used for pharmacokinetic investigations in the CNS, such data are unlikely to represent the pharmacodynamically relevant compartment, due to non-specific binding to brain lipids and proteins. The brain consists of extracellular, intracellular and cerebrospinal fluid (CSF) compartments, and the relevant compartment depends on where the drug acts. A high concentration of a drug in a brain tissue homogenate sample may only be viewed as an indication of good blood–brain barrier (BBB) penetration, and does not necessarily suggest high unbound drug concentrations at the target site [9]. Hence, a more detailed pharmacokinetic evaluation may be needed to interpret the pharmacodynamic outcome of *in vivo* behavioural or neurochemical studies of CNS-active compounds such as antidepressants, as well as to improve the experimental design of pharmacological animal models.

The recent advances within intracerebral microdialysis have enabled quantitative information about the unbound (free) drug concentrations at the extracellular target site in discrete areas of the rodent brain [10,11]. This technique has a temporal and spatial resolution suitable for the study of neuropharmacokinetics in the brain extracellular fluid (bECF) following peripheral drug administration. The unbound extracellular brain concentration measured by microdialysis may reflect the amount of drug available at the pharmacological target for, for example, receptor or transporter occupancy. Therefore, such data may facilitate the understanding of the temporal features of drug-induced pharmacological changes in a pharmacokinetic/pharmacodynamic context when extracellular drug levels and neurochemical or behavioural changes are determined simultaneously [12–14].

In addition, when the blood/plasma kinetics is assessed concurrently with the brain uptake and kinetics of the unbound drug, the transport rate and extent of equilibration across the BBB can be studied. By adapting such information into pharmacokinetic compartmental models, direct quantitative information about the *in vivo* net flux across the BBB and the possible influx and efflux mechanisms may be used in simulations at different dosing scenarios [15–17]. Few applications of such an approach have been described for antidepressant drugs. The present study sought to characterize the peripheral plasma pharmacokinetic and central bECF kinetic interrelationship of escitalopram by compartmental modelling. For this purpose, escitalopram was measured in rat plasma and bECF during and after different constant rate intravenous infusions using a validated freely moving rat model designed for simultaneous intracerebral microdialysis and serial blood sampling [18].

Materials and Methods

Chemicals

Escitalopram and a chlorine substituted internal standard (Lu 10-202) were provided by H. Lundbeck, A/S, Denmark. Escitalopram was used as oxalate salt dissolved in 0.9% NaCl. Filtered degassed artificial cerebrospinal fluid (aCSF) was used as the microdialysis perfusion fluid with the following composition: 145 mM NaCl, 3 mM KCl, 1 mM $MgCl_2$, 1.2 mM $CaCl_2$, pH adjusted to 7.0. All chemicals and solvents used were of analytical grade.

Animal preparation

Male Sprague-Dawley rats weighing 300–375 g were used. The animals were housed under a 12 h light/dark cycle under controlled conditions of regular indoor temperature ($21 \pm 2^{\circ}C$) and humidity ($55 \pm 5\%$) with food and tap water available *ad libitum*. The protocol was approved by the Animal Welfare Committee, appointed by the Danish Ministry of Justice and all animal procedures were carried out in compliance with EC Directive 86/609/EEC and with the Danish law regulating experiments on animals.

The pharmacokinetic experiments were conducted using a conscious, freely behaving rat model described previously [18]. Briefly, surgical preparation of the animals was carried out in two stages, each followed by a recovery period of 48 h. Implantation of intracerebral microdialysis probe guide cannulas was performed in the first stage followed by vascular catheterizations in the same animals, in the second stage. Under fluanisone (5 mg/kg), fentanyl (0.2 mg/kg) and

DOI: 10.1002/bdd

midazolam (2.5 mg/kg) anaesthesia, a guide cannula (CMA/12, CMA/Microdialysis, Sweden) was stereotaxically implanted aiming to position the dialysis probe tip in the ventral hippocampus according to the following coordinates: 5.6 mm posterior to bregma, lateral −5.0 mm, 7.0 mm ventral to dura [19]. After the recovery period, indwelling catheters (Tygon® S-50-HL, 0.4 mm i.d.; 0.79 mm o.d., Datainnovation AB, Sweden) were implanted in the external jugular vein and the common carotid artery according to standard surgical procedures [20,21]. After subcutaneous externalization, the arterial catheter was attached to a dual channel swivel (Instech 375/D/22, Instech Lab., PA, USA) allowing the animals to move freely within their cages during the experiment.

Experimental procedure

On the day of the experiment, a polycarbonate microdialysis probe (CMA/12, 0.5 mm diameter, 3 mm length) was slowly inserted through the guide cannula into the brain and perfused with aCSF at a flow rate of 2 μl/min using a syringe pump. Concomitantly, the arterial catheter was connected to an automated blood sampling system (AccuSampler™, Datainnovation AB) via the liquid swivel. After 180 min of stabilization, escitalopram was administered as a constant-rate intravenous infusion over 60 min. Rats were assigned to three groups of six, receiving 2.5, 5 or 10 mg/kg escitalopram. Dosing solutions were prepared so that actual infusion flow-rates were in the range of 5–15 μl/min, adjusted for body weight. Microdialysate fractions were collected every 20 min throughout the experiment. Arterial blood samples (100 or 200 μl depending on the dose) were drawn at pre-programmed time intervals at 10, 30, 50 and 60 min during infusion, and at 70, 80, 100, 120, 180, 240, 300 and 360 min after the start of infusion. An equal volume of sterile heparinized saline automatically replaced each blood sample withdrawn. The plasma was separated by centrifugation for 10 min (6500 *g*) and stored at −20°C together with the microdialysis samples until drug analysis. During blood and microdialysis sampling, all time points were corrected for lag time of the drug solution in the infusion catheter and of the perfusate from the microdialysis site to the probe outlet.

At completion of each pharmacokinetic experiment, the microdialysis probes were calibrated individually *in vivo* according to the method of retrodialysis by drug [22] by perfusing the probes with 50 ng/ml escitalopram dissolved in aCSF. *In vivo* recovery was calculated by the loss of escitalopram from the perfusion solution to the surrounding tissue according to the following equation:

$$\text{Recovery}_{in\ vivo}(\%) = \left(\frac{C_{\text{in}} - C_{\text{out}}}{C_{\text{in}}}\right) \times 100 \qquad (1)$$

where C_{in} is the escitalopram concentration entering the probe and C_{out} is the concentration leaving the probe. The concentrations of escitalopram in the brain extracellular fluid were calculated from the dialysate concentrations after adjustment for the *in vivo* recovery by the retrodialysis method. Conversion of escitalopram dialysate concentrations into absolute extracellular levels by means of this approach was verified previously by use of the no-net-flux method at steady state [23], which resulted in similar recovery estimates [18]. After the experiments were concluded, the animals were killed using an intravenous overdose of sodium pentobarbital.

Drug analysis

For the analysis of escitalopram, 20 μl of dialysate was directly injected into a high-performance liquid chromatography system (L-7000 Merck-Hitachi, Germany) equipped with an XTerra reverse phase narrow bore column (150 × 2.1 mm i.d., 3.5 μm particles, Waters, MA, USA) and a fluorescence detector. Emission of the analyte was monitored at 296 nm, with excitation at 240 nm. Elution was performed at 30°C using a mobile phase consisting of 44 mM phosphate buffer containing 0.1% triethyl amine (pH 4.5):acetonitrile (71:29 v/v). The flow-rate was set to 0.2 ml/min. Based on a signal-to-noise (S/N) ratio of 3:1, the detection limit was 0.5 ng/ml and linear calibration curves were constructed from the detection limit to 100 ng/ml.

Escitalopram concentrations in plasma were determined using the same chromatographic system as described above, but with a Hypersil

DOI: 10.1002/bdd

C_{18} column (200 mm × 4.6 mm i.d., 5 μm particles, Agilent, CA, USA). The mobile phase consisted of 44 mM phosphate buffer (pH 4.5) and acetonitrile (55:45 v/v) delivered at a flow rate of 1.2 ml/min. Prior to injection, the plasma samples were purified by a two-step liquid–liquid extraction procedure described previously [18,24]. A chlorine substituted internal standard was added to all plasma samples before the extraction procedure. Using this assay method, the limit of detection was 1.6 ng/ml using 50 μl plasma (S/N ratio = 3). Linear calibration curves were established from 2 to 600 ng/ml escitalopram.

Pharmacokinetic analysis

Prior to the pharmacokinetic analysis, total escitalopram plasma concentrations were converted into unbound concentrations by correcting for a mean protein binding of 50% (range 45–55%), determined in Sprague-Dawley rat plasma using *in vitro* ultrafiltration, exhibiting concentration-independent binding in the range 30–1000 ng/ml (H. Lundbeck A/S, unpublished data). A protein binding of 50% was also obtained in spiked plasma samples containing 50 ng/ml escitalopram taken from rats equipped with indwelling arterial and venous catheters for 3 days indicating a lack of effect of the surgical interventions on the protein binding of escitalopram.

All modelling procedures were performed using WinNonlin nonlinear regression software (vers. 4.1, Pharsight Corp, Mountain View, CA, USA). The area under the plasma or bECF concentration versus time curve ($AUC_{u,plasma}$, AUC_{bECF}) was estimated using a non-compartmental method. The AUC_{0-t} was calculated by the linear trapezoidal method and the residual area ($AUC_{t-\infty}$) was determined as the ratio of the observed concentration at the last time point to the corresponding terminal rate constant. $AUC_{0-\infty}$ was expressed as the sum of AUC_{0-t} and $AUC_{t-\infty}$.

In the compartmental modelling, unbound plasma and bECF escitalopram concentrations were analysed simultaneously, and the differential equations were parameterized in terms of intercompartmental rate constants and distribution volumes (Figure 1). The model was derived from a two-compartment open model connected to a brain compartment via the central compartment [16,25]. The general differential equation system associated with the transport processes depicted in Figure 1 were as follows:

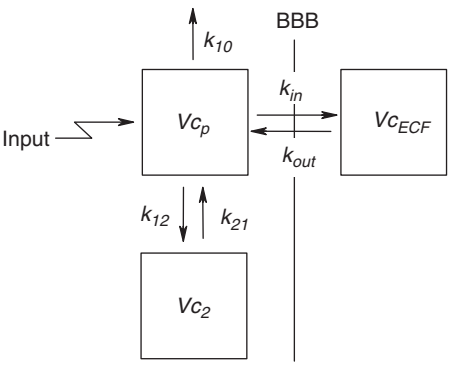

Figure 1. Compartmental model of escitalopram plasma disposition and drug exchange between plasma and brain extracellular fluid following intravenous infusion (input). Vc_p and Vc_{ECF} are volumes of distribution in the sampled plasma and brain extracellular compartment and Vc_2 is the volume of distribution in the peripheral tissue. k_{12}, k_{21} and k_{10} are plasma intercompartmental transfer rate constants and the elimination rate constant in the two-compartment open model. k_{in} and k_{out} signifies the intercompartmental transfer rate constants across the BBB

$$\frac{dC_p}{dt} = (inp/Vc_p) + k_{21}C_2(Vc_2/Vc_p) + k_{out}C_{ECF}(Vc_{ECF}/Vc_p) - C_p(k_{10} + k_{12} + k_{in}) \quad (2)$$

$$\frac{dC_2}{dt} = k_{12}C_p(Vc_p/Vc_2) - k_{21}C_2 \quad (3)$$

$$\frac{dC_{ECF}}{dt} = k_{in}C_p(Vc_p/Vc_{ECF}) - k_{out}C_{ECF} \quad (4)$$

where C_p and C_2 represents the drug concentrations in the central and peripheral plasma compartments and C_{ECF} is the extracellular concentration in the brain (see also Figure 1). *inp* signifies the input (administered dose). As k_{10} was found to be dose-dependent in a linear fashion, this parameter was expressed as a function of dose by linear regression as:

$$k_{10} = ITC + S \cdot Dose \quad (5)$$

DOI: 10.1002/bdd

where *ITC* and *S* correspond to the *y*-intercept and slope in the regression of k_{10} versus dose. In the final model, *ITC* and *S* were estimated as primary parameters substituting for k_{10} in Equation (2). Subsequently, k_{10} was calculated for each dose as secondary parameters from Equation (5).

The other secondary pharmacokinetic parameters derived from the final primary parameter estimates included distribution volume in the peripheral compartment (Vc_2), elimination half-life ($t_{1/2,\beta}$) and unbound clearances (CL_u) associated with elimination and intercompartmental distribution according to Equations (6)–(11) [26]:

$$Vc_2 = (k_{12}Vc_p)/k_{21} \tag{6}$$

$$\beta = \tfrac{1}{2}((k_{12} + k_{21} + k_{10}) - \sqrt{(k_{12} + k_{21} + k_{10})^2 - 4k_{21}k_{10}}) \tag{7a}$$

$$t_{1/2,\beta} = \ln 2/\beta \tag{7b}$$

$$CL_u = k_{10}Vc_p \tag{8}$$

$$CL_d = k_{12}Vc_p \tag{9}$$

$$CL_{in} = k_{in}Vc_p \tag{10}$$

$$CL_{out} = k_{out}Vc_{ECF} \tag{11}$$

Modelling was performed using data from all three doses simultaneously to characterize the integrated pharmacokinetic parameters over the entire dose range. As the initial analysis indicated dose-dependent kinetics related to k_{10}, this was accounted for by allowing the estimation of specific parameters affected by dose according to Equation (5). Dose-dependent parameters were indicated from separate compartmental analyses of data from each individual dose. The modelling analysis was based on mean concentrations from all rats at each time point in order to reduce the influence of random fluctuations in concentrations on model fit. A constant relative error model (weight proportional to the inverse of the squared predicted value) was used for weighting of data. Model selection was based on the Akaike information criterion (AIC) [27], random distribution of residuals and from the coefficients of variation (CV%) associated with each parameter estimate.

Results

In vivo recovery of escitalopram across the microdialysis membrane determined in each animal by retrodialysis averaged $17.9 \pm 5.4\%$ (SD, $n = 18$) at the applied perfusion flow rate of 2 µl/min. Continuous measurement of the loss of escitalopram from the perfusate under these conditions has previously shown that *in vivo* recovery of this compound is stable for up to 8 h [18]. *In vivo* retrodialysis was therefore considered reliable over the experimental period of the present pharmacokinetic studies.

Plots of average unbound escitalopram concentrations in plasma and bECF of the hippocampus versus time at the three tested doses are shown in Figure 2. Following intravenous infusion, escitalopram was rapidly transported across the BBB and distributed into the bECF. The change in bECF escitalopram concentrations during and after drug infusion was adequately captured by the temporal dialysis resolution of 20 min. After the end of the infusions, the unbound concentrations of escitalopram in brain and plasma decreased with the same half-life. The rapid attainment of equilibrium and the high distribution of escitalopram into the bECF was reflected in the ratios between AUC_{bECF} and $AUC_{u,plasma,}$ which amounted to 0.78 ($\pm$0.28), 0.76 ($\pm$0.16) and 0.86 ($\pm$0.18) (mean $\pm$ SD) at doses of 2.5, 5 and 10 mg/kg, respectively, calculated by non-compartmental analysis.

Plotting the dose-normalized *AUC*s for unbound plasma and bECF concentrations of escitalopram versus dose showed increasing values with dose and comparable slopes for both plasma and bECF exposure (Figure 3A). This indicated a non-linear dose-dependent disposition of escitalopram related to a decrease in systemic CL_u at higher doses. Consequently, as

DOI: 10.1002/bdd

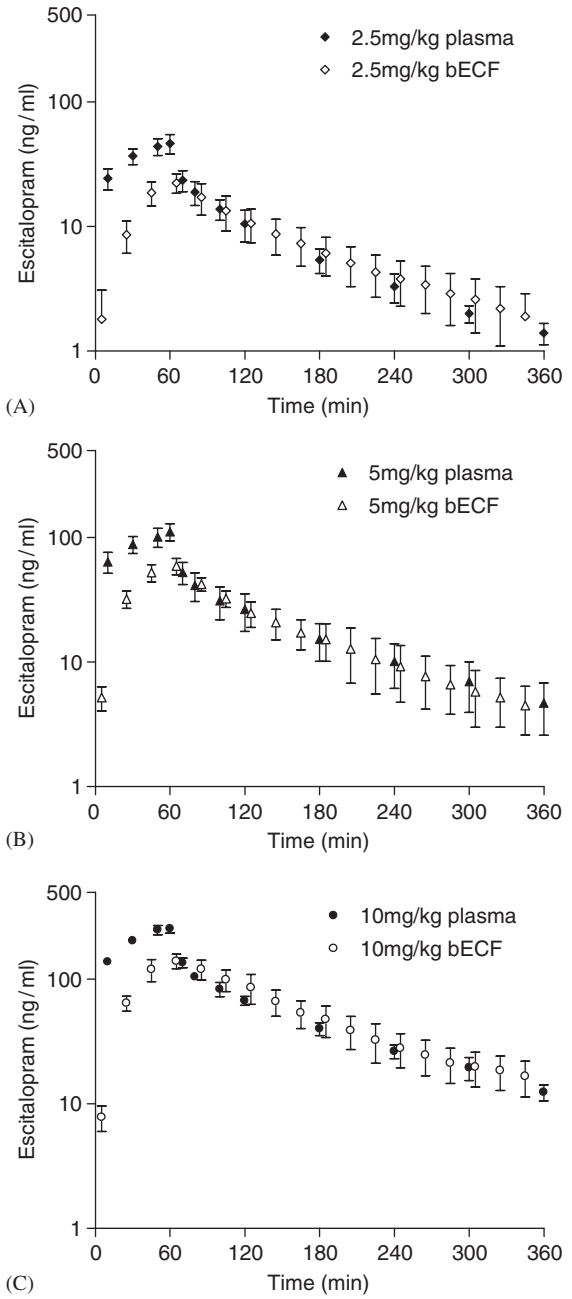

Figure 2. Semilogarithmic plots of unbound plasma and brain extracellular fluid escitalopram concentration versus time following 60 min constant rate intravenous infusion of 2.5 mg/kg (A), 5 mg/kg (B), and 10 mg/kg (C). Data are presented as mean ± SD ($n = 6$ rats per group)

illustrated in Figure 3B, k_{10} was shown to decrease with increasing doses following separate compartmental modelling of unbound plasma and brain concentrations from each dose level. Accordingly, characterizing the global pharmacokinetics by compartmental modelling using one set of primary parameters covering the entire dose range by fitting unbound plasma and brain data simultaneously from all doses to Equations (2)–(4) was not adequate to describe the experimental data. The pharmacokinetic fit obtained by using this approach is shown in Figure 4.

To account for the decreases in k_{10} with increasing doses, the plasma and brain data were simultaneously reanalysed using Equations (2)–(5) by incorporating a linear dose-dependency of k_{10}. During this analysis, global estimates of the remaining parameters covering the entire dose range were allowed. The ability of this model to account for the dose-dependency was evident from the close agreement of the model-calculated profiles shown in Figure 5 with the experimental data. Thus, a two-compartment model with variable k_{10} best described the pharmacokinetics of escitalopram in plasma, whereas a one-compartment model was sufficient to characterize the disposition in the bECF. The resulting parameter estimates from the final analysis are listed in Table 1, which describe the plasma and bECF concentration versus time curves at all infusion doses. The calculated parameter estimates showed low correlation and had acceptable precision expressed as coefficients of variation (CV%), which were below 16%. Using Equations (10) and (11), the influx and efflux clearances across the BBB (CL_{in} and CL_{out}) were calculated as 535 and 666 µl/min/g brain. The ratio between CL_{in} and CL_{out} (~0.80) was thus in close agreement with the brain/plasma distribution ratios obtained based on the *AUC*s of unbound plasma and bECF escitalopram concentrations (0.76–0.86).

A saturable two-compartment model with Michaelis-Menten elimination kinetics was evaluated to fit simultaneously the three plasma and bECF concentration-time profiles. This analysis, however, resulted in systematic deviations between predicted and observed data and gave imprecise and highly correlated parameters, and was therefore not applied. Due to the fast drug transfer observed for escitalopram across

DOI: 10.1002/bdd

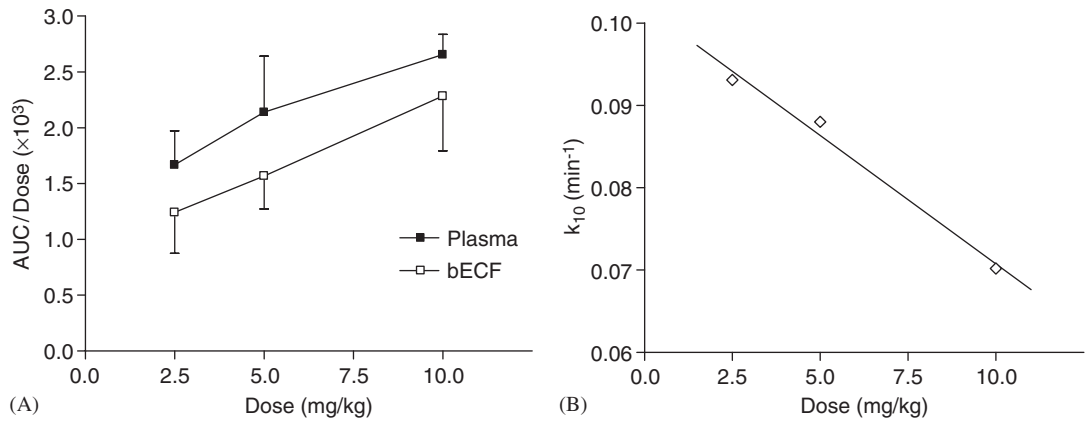

Figure 3. (A) Plot of dose-normalized $AUC_{0-\infty}$ for escitalopram in plasma and brain extracellular fluid versus the three investigated doses (2.5, 5 and 10 mg/kg) illustrating the non-linear disposition of escitalopram. Data shown as mean ± SD ($n = 6$ rats per group). (B) Plot and linear regression of calculated estimates of k_{10} after individual compartmental analyses at each individual dose ($r^2 = 0.986$)

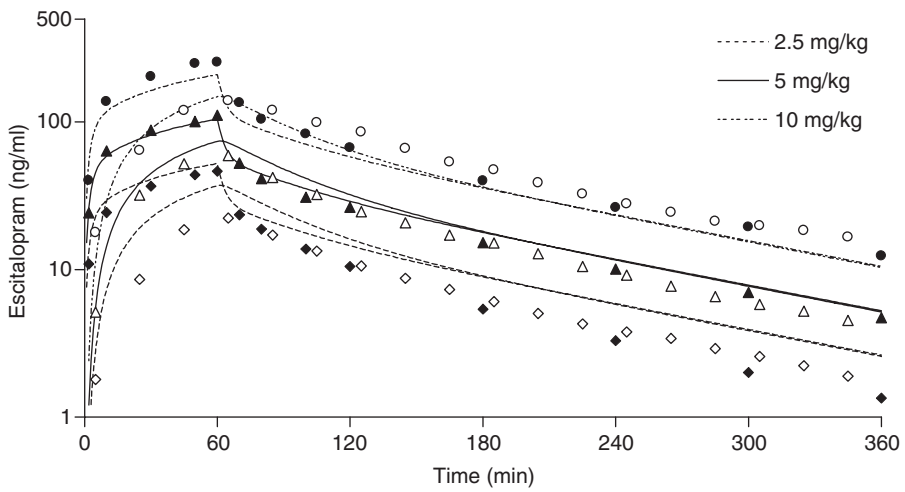

Figure 4. Measured (mean) concentration-time courses of unbound escitalopram in plasma and brain extracellular fluid following intravenous administration of 2.5, 5 and 10 mg/kg and corresponding model-fitted concentration-time profiles. Pharmacokinetic modelling was performed simultaneously on mean data from all doses using a single estimate of each pharmacokinetic parameter over the entire dose-range (Equations (2)–(4)). Symbols as in Figure 2

the BBB during infusion, a 'brain-infusion' pharmacokinetic model was also tested, in which k_{in} was assumed to be similar to the input (infusion dose), corrected for protein binding. However, this approach also gave rise to systematic deviations in the model output (weighted residual concentrations versus time) and resulted in higher AIC values when data from all doses were analysed simultaneously (data not shown).

In order to evaluate the final pharmacokinetic model of the plasma and brain kinetic interrelationship, a simulation was conducted by changing the mode of administration of escitalopram. Thus, the applicability of the model was tested by simulating an intravenous bolus injection of 2.5 mg/kg escitalopram as model input and applying the final parameter estimates in Table 1. The predicted unbound plasma and bECF concentration-time profiles following this

DOI: 10.1002/bdd

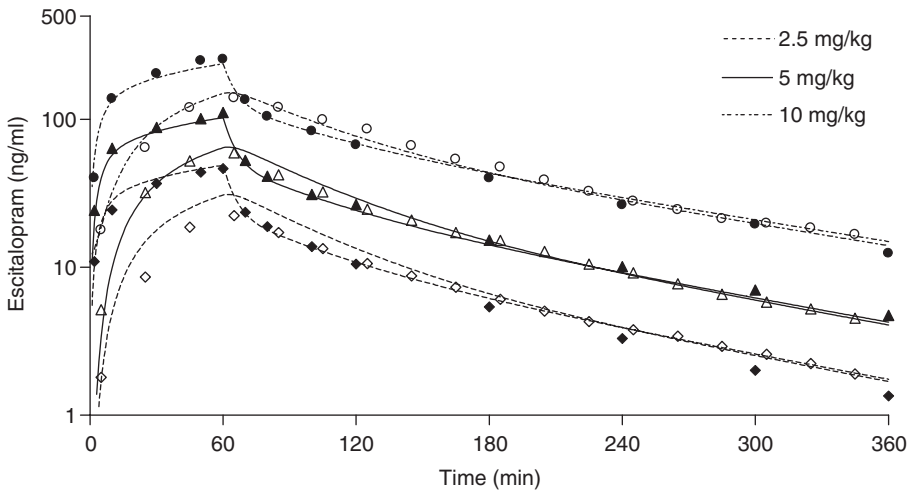

Figure 5. Measured (mean) and model-fitted unbound escitalopram concentration-time profiles in plasma and brain extracellular fluid following intravenous administration of 2.5, 5 and 10 mg/kg. Pharmacokinetic modelling was performed simultaneously on mean data from all doses by Equations (2)–(5) allowing a dose-dependent estimation of k_{10} expressed by Equation (5). Symbols as in Figure 2

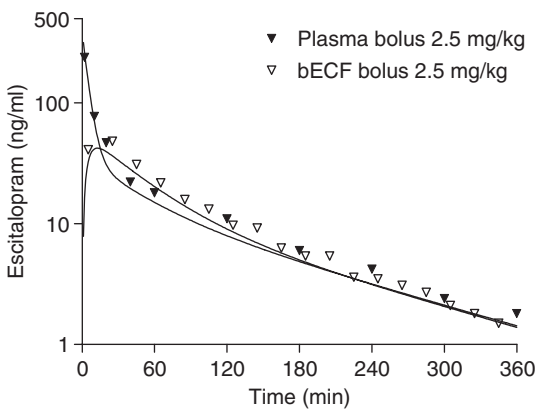

Figure 6. Simulation (solid lines) of unbound plasma and brain extracellular fluid escitalopram concentrations using the final pharmacokinetic parameter estimates applied to an intravenous bolus injection pharmacokinetic model using 2.5 mg/kg as model input. Symbols represent measured unbound escitalopram concentrations in plasma and brain extracellular fluid following intravenous bolus administration of 2.5 mg/kg in a representative rat

procedure are depicted in Figure 6. Actual plasma and bECF concentrations measured at regular time-points after intravenous bolus injection of 2.5 mg/kg of escitalopram are shown in the same figure for comparison. Although the model tended to underpredict plasma and bECF concentrations to some degree, the rapid equilibrative distributional behaviour of escitalopram between plasma and brain was adequately predicted based on the 60 min intravenous infusion data.

Discussion

This study was designed to investigate the pharmacokinetics of escitalopram including its temporal plasma-brain kinetic inter-relationship in conscious rats by using intracerebral microdialysis in conjunction with regular blood sampling. There are some reports of antidepressant drug disposition in rat brain using microdialysis [28–33]. However, the quantitative pharmacokinetic information from these studies is limited, due to a lack of correction for microdialysis probe recovery *in vivo*, an insufficient duration of the experiment to describe fully the distribution and elimination of the drug under investigation, or a lack of analytical sensitivity. This study sought to characterize fully the pharmacokinetics of escitalopram in brain and plasma by compartmental modelling using a validated microdialysis rat model suited for such purpose.

Whereas non-compartmental modelling of plasma and brain concentration-time data only

DOI: 10.1002/bdd

Table 1. Pharmacokinetic parameter estimates obtained by simultaneous modelling of mean unbound plasma and bECF concentrations of escitalopram after intravenous infusion of 2.5, 5, and 10 mg/kg to rats. A global fitting procedure covering the entire dose range was performed, resulting in a single estimate for each pharmacokinetic parameter with the exception of k_{10}, which was expressed by *S* and *ITC* as a linear function of dose. Secondary parameters calculated for the applied doses of 2.5, 5 and 10 mg/kg correspond to low, med and high, respectively. Coefficients of variation (CV%) reflect the precision of the obtained parameter estimates

Primary parameter	Estimate ± CV (%)	Secondary parameter[a]	Estimate ± CV (%)
k_{in} (min^{-1})	0.078 ± 16	Vc_2 (l/kg)	24.6 ± 7
k_{out} (min^{-1})	0.039 ± 6	CL_d (l/min/kg)	0.27 ± 11
k_{12} (min^{-1})	0.039 ± 12	CL_{in} (µl/min/g)	535 ± 13
k_{21} (min^{-1})	0.011 ± 12	CL_{out} (µl/min/g)	666 ± 12
Vc_p (l/kg)	6.84 ± 7	$k_{10,low}$ (min^{-1})	0.078 ± 7
Vc_{ECF} (ml/g)	17.0 ± 8	$k_{10,med}$ (min^{-1})	0.071 ± 7
S (mg/kg min × 10^{-3})	−2.70 ± 10	$k_{10,high}$ (min^{-1})	0.058 ± 8
ITC (min^{-1})	0.085 ± 7	$CL_{u,low}$ (l/min/kg)	0.54 ± 2
		$CL_{u,med}$ (l/min/kg)	0.49 ± 3
		$CL_{u,high}$ (l/min/kg)	0.39 ± 3
		$t_{1/2,low}$ (min)	98 ± 9
		$t_{1/2,med}$ (min)	103 ± 9
		$t_{1/2,high}$ (min)	112 ± 8

[a]Calculated according to Equations (6)–(11).

measures the extent of net BBB transport, compartmental modelling enables both the rate and the extent of transport to be estimated. In studies of BBB transport of drugs, both the rate and the extent of transport need to be considered. These characteristics will affect the degree, onset and duration of the centrally mediated effect. The rate of drug transport across the BBB is related to the physico-chemical properties of the drug, whereas the extent of equilibration is also influenced by the involvement of active membrane transport mechanisms located at the endothelial cells in the BBB. In this study, escitalopram rapidly entered the bECF following acute intravenous infusion. Based on the proposed pharmacokinetic model, the unbound CL_{in} into the bECF for escitalopram was estimated to be 535 µl/min/g brain. This value is much higher than influx clearances into the bECF of rats found for other CNS active compounds such as morphine (11 µl/min/g) [15] and gabapentin (44 µl/min/g) [17]. However, drugs exhibiting higher extraction into rat brain than escitalopram have also been reported, for example the opioid agonist oxycodone, with a CL_{in} value of 1900 µl/min/g brain [34]. The CL_{out} for escitalopram was estimated to be 666 µl/min/g brain, which was in the same range as for the CL_{in}. Thus, based on the CL_{in}/CL_{out} ratio (0.80), no clear indication of active efflux or influx processes across the BBB could be identified for escitalopram.

The BBB transport mechanisms of the racemate citalopram, which comprises the S(+)-enantiomer (escitalopram) and the R(−)-enantiomer, have been investigated by different *in vitro* and *in vivo* methods. Transport studies using monolayers of bovine brain microvessel endothelial cells, suggests that citalopram crosses the BBB by means of a saturable, non-stereoselective, carrier-mediated mechanism [35]. In addition, recent *in vivo* brain uptake studies performed in genetically modified P-gp knock out mice, showed that the brain exposure of citalopram was improved 2–3 fold in mice lacking P-gp compared with wild-type controls, suggesting that citalopram could be a substrate for P-gp in this species [36,37]. A stereoselective analysis of brain homogenates after acute administration of citalopram in rats has shown that peak levels of the R- and S-enantiomers do not differ significantly, indicating non-stereoselectivity in the BBB influx and efflux processes [38]. Thus, according to the published data, it cannot be ruled out that both active brain influx and efflux participate in the net BBB transport of escitalopram. However,

DOI: 10.1002/bdd

our findings suggest that neither of these putative active mechanisms are significant *in vivo* and points toward predominantly passive bi-directional transport. Furthermore, a single estimate of k_{in}, covering the entire dose range, was adequate to characterize the influx of escitalopram to the brain. Thus, no indication of a saturable brain influx of escitalopram was observed within the dose range tested in these experiments.

Compared with the pharmacokinetics of R,S-citalopram previously reported in rats [39], escitalopram exhibited a higher systemic clearance and a shorter half-life in plasma. This might be explained by a more rapid demethylation of escitalopram compared with R-citalopram, as found both *in vitro* and *in vivo* [38,40]. In addition, an apparent dose-dependency of the systemic clearance of escitalopram was found. Thus, incorporation of the individual estimates of k_{10} for each dose level into the simultaneous modelling procedure resulted in the successful characterization of the pharmacokinetics over the entire dose range. Simulation studies were conducted to test the usefulness and predictability of the pharmacokinetic model. The model allowed a reasonable prediction of the time profiles of escitalopram concentrations in plasma and bECF following other treatment regimens, exemplified by an intravenous bolus administration of escitalopram. Thus, such pharmacokinetic simulations for different dosing scenarios may be valuable in terms of the design and interpretation of pharmacological *in vivo* studies.

The pharmacokinetic analysis of escitalopram resulted in an estimate of the unbound volume of distribution in the brain (Vc_{ECF}) of 17 ml/g brain, thus greatly exceeding the brain extracellular space reported to be 0.15–0.20 ml/g brain in rats [41]. This suggests that escitalopram is highly distributed intracellularly in the brain and/or binds readily to tissue components in the extracellular space. This is substantiated by previous findings that demonstrate high total brain/plasma exposure ratios of escitalopram following peripheral administration in rats [4,38]. Also, the Vc_{ECF} of 17 ml/g brain estimated by our pharmacokinetic modelling approach corresponds closely to unbound and total brain concentration data obtained for citalopram following chronic administration in rats [31]. Thus, total brain (A_{br}) and bECF concentrations (C_{bECF}) at steady-state of approximately 200 ng/g and 10 ng/ml have been reported using subcutaneous osmotic pumps [31]. Accordingly, Vc_{ECF} may be approximated by A_{br}/C_{bECF}, corresponding to 20 ml/g brain, which is in the same range as estimated in our study using the compartmental modelling approach. The high total brain concentrations reported are also consistent with the high volume of distribution in the plasma compartments found in the current study.

A prerequisite for applying intracerebral microdialysis for studying BBB transport and drug disposition within the brain is that the BBB characteristics will not be significantly influenced by microdialysis probe implantation and presence in the brain. Microdialysis, characterized as a minimal invasive technique, causes unavoidable local tissue trauma, followed by transient perturbation of the BBB function [42]. However, based on studies performed to evaluate the usefulness of intracerebral microdialysis in assessment of passive as well as active BBB transport in rats, the BBB appears to function normally in the presence of the dialysis probe [17,43–46]. In addition, when intracerebral microdialysis is applied for quantitative purposes such as studies of BBB drug transport, the probe calibration procedure should be appropriately validated, to ensure that a reliable estimate of recovery across the probe membrane is obtained. The method of *in vivo* retrodialysis, used in the current study, has recently been validated against the more accurate, but more time-consuming method of no-net-flux, which showed similar recovery estimates for escitalopram between the two methods [18]. *In vivo* retrodialysis may therefore accurately facilitate conversion of dialysate concentrations of escitalopram into absolute extracellular concentrations in the brain. Thus, provided that intracerebral microdialysis is used under well-controlled surgical and experimental conditions this technique is considered suitable for studies of BBB transport and neuropharmacokinetics.

In conclusion, the use of intracerebral microdialysis in conjunction with automated blood sampling provided data suitable for studying plasma and brain pharmacokinetics of escitalopram

DOI: 10.1002/bdd

in rats. The pharmacokinetic inter-relationship between plasma and extracellular space in the brain and the associated transport processes could be described using a compartmental modelling procedure which simultaneously quantified the global pharmacokinetic parameters over the entire dose range, together with the dose-dependent pharmacokinetic parameters. By modelling the bi-directional distribution in and out of the brain, these results are representative of the process that determines the time course of drug effect in the experimental animal. Thus, such models may be valuable in the interpretation and design of preclinical *in vivo* pharmacological studies.

Conflict of Interest Statement

The authors are employed at H. Lundbeck A/S, R&D.

References

1. Baldwin DS, Cooper JA, Huusom AK, Hindmarch I. A double-blind, randomized, parallel-group, flexible-dose study to evaluate the tolerability, efficacy and effects of treatment discontinuation with escitalopram and paroxetine in patients with major depressive disorder. *Int Clin Psychopharmacol* 2006; **21**: 159–169.
2. Sánchez C. The pharmacology of citalopram enantiomers: the antagonism by R-citalopram on the effect of S-citalopram. *Basic Clin Pharmacol Toxicol* 2006; **99**: 91–95.
3. Stein DJ, Andersen EW, Lader M. Escitalopram versus paroxetine for social anxiety disorder: an analysis of efficacy for different symptom dimensions. *Eur Neuropsychopharmacol* 2006; **16**: 33–38.
4. Ceglia I, Acconcia S, Fracasso C, Colovic M, Caccia S, Invernizzi RW. Effects of chronic treatment with escitalopram or citalopram on extracellular 5-HT in the prefrontal cortex of rats: role of 5-HT_{1A} receptors. *Br J Pharmacol* 2004; **42**: 469–478.
5. Fish EW, Faccidomo S, Gupta S, Miczek KA. Anxiolytic-like effects of escitalopram, citalopram, and R-citalopram in maternally separated mouse pups. *J Pharmacol Exp Ther* 2004; **308**: 474–480.
6. Sánchez C, Bergqvist PB, Brennum LT, *et al*. Escitalopram, the S-(+)-enantiomer of citalopram, is a selective serotonin reuptake inhibitor with potent effects in animal models predictive of antidepressant and anxiolytic activities. *Psychopharmacology* 2003; **167**: 353–362.
7. de Lange EC, Ravenstijn PG, Groenendaal D, van Steeg TJ. Toward the prediction of CNS drug-effect profiles in physiological and pathological conditions using microdialysis and mechanism-based pharmacokinetic–pharmacodynamic modelling. *AAPS J* 2005; **7**: E532–E543.
8. Walker MC, Tong X, Perry H, Alavijeh MS, Patsalos PN. Comparison of serum, cerebrospinal fluid and brain extracellular fluid pharmacokinetics of lamotrigine. *Br J Pharmacol* 2000; **130**: 242–248.
9. Lin JH. Tissue distribution and pharmacodynamics: a complicated relationship. *Curr Drug Metab* 2006; **7**: 39–65.
10. Cano-Cebrian MJ, Zornoza T, Polache A, Granero L. Quantitative *in vivo* microdialysis in pharmacokinetic studies: some reminders. *Curr Drug Metab* 2005; **6**: 83–90.
11. Hammarlund-Udenaes M. The use of microdialysis in CNS drug delivery studies. Pharmacokinetic perspectives and results with analgesics and antiepileptics. *Adv Drug Deliv Rev* 2000; **45**: 283–294.
12. Weikop P, Egestad B, Kehr J. Application of triple-probe microdialysis for fast pharmacokinetic/pharmacodynamic evaluation of dopamimetic activity of drug candidates in the rat brain. *J Neurosci Methods* 2004; **140**: 59–65.
13. Bouw MR, Gårdmark M, Hammarlund-Udenaes M. Pharmacokinetic-pharmacodynamic modelling of morphine transport across the blood–brain barrier as a cause of the antinociceptive effect delay in rats—a microdialysis study. *Pharm Res* 2000; **17**: 1220–1227.
14. Clausing P, Bloom D, Newport GD, Holson RR, Slikker Jr W, Bowyer JF. Individual differences in dopamine release but not rotational behavior correlate with extracellular amphetamine levels in caudate putamen in unlesioned rats. *Psychopharmacology* 1996; **127**: 187–194.
15. Tunblad K, Jonsson EN, Hammarlund-Udenaes M. Morphine blood–brain barrier transport is influenced by probenecid co-administration. *Pharm Res* 2003; **20**: 618–623.
16. Hammarlund-Udenaes M, Paalzow LK, de Lange EC. Drug equilibration across the blood–brain barrier—pharmacokinetic considerations based on the microdialysis method. *Pharm Res* 1997; **14**: 128–134.
17. Wang Y, Welty DF. The simultaneous estimation of the influx and efflux blood–brain barrier permeabilities of gabapentin using a microdialysis–pharmacokinetic approach. *Pharm Res* 1996; **13**: 398–403.
18. Bundgaard C, Jørgensen M, Mørk A. An integrated microdialysis rat model for multiple pharmacokinetic/pharmacodynamic investigations of serotonergic agents. *J Pharmacol Toxicol Methods* 2007; **55**: 214–223.
19. Paxinos G, Watson C. *The Rat Brain in Stereotaxic Coordinates*. Academic Press: San Diego, 1986.
20. Thrivikraman KV, Huot RL, Plotsky PM. Jugular vein catheterization for repeated blood sampling in the unrestrained conscious rat. *Brain Res Protoc* 2002; **10**: 84–94.
21. Van Dongen JJ, Remie R, Rensema JW, van Wunnik GHJ. *Manual of Microsurgery on the Laboratory Rat*. Elsevier: Maastricht, 1990.
22. Bouw MR, Hammarlund-Udenaes M. Methodological aspects of the use of a calibrator in *in vivo* microdialysis—further development of the retrodialysis method. *Pharm Res* 1998; **15**: 1673–1679.

DOI: 10.1002/bdd

23. Lönnroth P, Jansson PA, Smith U. A microdialysis method allowing characterization of intercellular water space in humans. *Am J Physiol* 1987; **253**: E228–E231.
24. Sidhu J, Priskorn M, Poulsen M, Segonzac A, Grollier G, Larsen F. Steady-state pharmacokinetics of the enantiomers of citalopram and its metabolites in humans. *Chirality* 1997; **9**: 686–692.
25. Chenel M, Marchand S, Dupuis A, *et al*. Simultaneous central nervous system distribution and pharmacokinetic–pharmacodynamic modelling of the electroencephalogram effect of norfloxacin administered at a convulsant dose in rats. *Br J Pharmacol* 2004; **142**: 323–330.
26. Gabrielsson J, Weiner D. *Pharmacokinetic and Pharmacodynamic Data Analysis*: *Concepts and Applications* (3rd edn). Swedish Pharmaceutical Press: Stockholm, 2000.
27. Yamaoka K, Nakagawa T, Uno T. Application of Akaike's information criterion (AIC) in the evaluation of linear pharmacokinetic equations. *J Pharmacokinet Biopharm* 1978; **6**: 165–175.
28. Fukushima T, Naka-aki E, Guo XJ, *et al*. Determination of fluoxetine and norfluoxetine in rat brain microdialysis samples following intraperitoneal fluoxetine administration. *Anal Chim Acta* 2004; **522**: 99–104.
29. Mørk A, Kreilgaard M, Sánchez C. The R-enantiomer of citalopram counteracts escitalopram-induced increase in extracellular 5-HT in the frontal cortex of freely moving rats. *Neuropharmacology* 2003; **45**: 167–173.
30. Cheng FC, Tsai TH, Wu YS, Kuo JS, Chen CF. Pharmacokinetic and pharmacodynamic analyses of trazodone in rat striatum by *in vivo* microdialysis. *J Pharm Biomed Anal* 1999; **19**: 293–300.
31. Wikell C, Apelqvist G, Carlsson B, *et al*. Pharmacokinetic and pharmacodynamic responses to chronic administration of the selective serotonin reuptake inhibitor citalopram in rats. *Clin Neuropharmacol* 1999; **22**: 327–336.
32. Wikell C, Bergqvist PB, Hjorth S, Apelqvist G, Bjork H, Bengtsson F. Brain monoamine output alterations after a single venlafaxine challenge in experimental hepatic encephalopathy. *Clin Neuropharmacol* 1998; **21**: 296–306.
33. Sato Y, Shibanoki S, Sugahara M, Ishikawa K. Measurement and pharmacokinetic analysis of imipramine and its metabolite by brain microdialysis. *Br J Pharmacol* 1994; **112**: 625–629.
34. Boström E, Simonsson US, Hammarlund-Udenaes M. *In vivo* blood–brain barrier transport of oxycodone in the rat: indications for active influx and implications for pharmacokinetics/pharmacodynamics. *Drug Metab Dispos* 2006; **34**: 1624–1631.
35. Rochat B, Baumann P, Audus KL. Transport mechanisms for the antidepressant citalopram in brain microvessel endothelium. *Brain Res* 1999; **831**: 229–236.
36. Doran A, Obach RS, Smith BJ, *et al*. The impact of P-glycoprotein on the disposition of drugs targeted for indications of the central nervous system: evaluation using the MDR1A/1B knockout mouse model. *Drug Metab Dispos* 2005; **33**: 165–174.
37. Uhr M, Grauer MT. abcb1ab P-glycoprotein is involved in the uptake of citalopram and trimipramine into the brain of mice. *J Psychiatr Res* 2003; **37**: 179–185.
38. Kugelberg FC, Carlsson B, Ahlner J, Bengtsson F. Stereoselective single-dose kinetics of citalopram and its metabolites in rats. *Chirality* 2003; **15**: 622–629.
39. Cremers TIFH, de Boer P, Liao Y, *et al*. Augmentation with a 5-HT_{1A}, but not a 5-HT_{1B} receptor antagonist critically depends on the dose of citalopram. *Eur J Pharmacol* 2000; **397**: 63–74.
40. Olesen OV, Linnet K. Studies on the stereoselective metabolism of citalopram by human liver microsomes and cDNA-expressed cytochrome P450 enzymes. *Pharmacology* 1999; **59**: 298–309.
41. Rosenberg GA, Kyner WT, Estrada E. Bulk flow of brain interstitial fluid under normal and hyperosmolar conditions. *Am J Physiol* 1980; **238**: F42–F49.
42. Clapp-Lilly KL, Roberts RC, Duffy LK, Irons KP, Hu Y, Drew KL. An ultrastructural analysis of tissue surrounding a microdialysis probe. *J Neurosci Methods* 1999; **90**: 129–142.
43. de Lange EC, Marchand S, van den Berg D, *et al*. *In vitro* and *in vivo* investigations on fluoroquinolones; effects of the P-glycoprotein efflux transporter on brain distribution of sparfloxacin. *Eur J Pharm Sci* 2000; **12**: 85–93.
44. Xie R, Bouw MR, Hammarlund-Udenaes M. Modelling of the blood–brain barrier transport of morphine-3-glucuronide studied using microdialysis in the rat: involvement of probenecid-sensitive transport. *Br J Pharmacol* 2000; **131**: 1784–1792.
45. Xie R, Hammarlund-Udenaes M. Blood–brain barrier equilibration of codeine in rats studied with microdialysis. *Pharm Res* 1998; **15**: 570–575.
46. Desrayaud S, Guntz P, Scherrmann JM, Lemaire M. Effect of the P-glycoprotein inhibitor, SDZ PSC 833, on the blood and brain pharmacokinetics of colchicine. *Life Sci* 1997; **61**: 153–163.

DOI: 10.1002/bdd